Spectral Radiant Intensity Calculation of Air in Shock Tube

Jun Ming Lyu, X. L. Cheng, J. J. Yu, F. Li, and X. L. Yu

Abstract Radiative heat may be greater than convective heat when flying at the velocity above 10 km/s. It is critical to precisely predict radiative heat for thermal protection system design. High-enthalpy flowfield solving and gas species' radiant coefficient calculation are two main contents in computing radiation heat. A series of tests to obtain quantitative emission spectral radiation of air at high velocity have been conducted in a detonation-driven shock tube. Based on optical calibration and measurement, volumetric spectral radiant intensities of N_2 and air have been acquired in the spectrum range of 310–380 nm and in the velocity range of 5.5–8 km/s. Unsteady non-equilibrium Navier-Stokes equations were numerically solved for temperature and gas concentration in the shock tube under test conditions. A narrowband model was used to calculate the gas spectral intensity at the specific position behind the shock corresponding to test time delay. The comparison between the computational results and the test measurement shows that the predictions of the flowfield parameters and the gas spectral radiation intensities are accurate and reliable.

1 Introduction

When vehicles reenter into Earth's atmosphere at hyper velocity, high-temperature gas in shock layer undergoes strong physical and chemical change, along with substantive gas radiation. Radiative heat will increase extremely fast along with the velocity goes up, may even be greater than convective heat when flying at the velocity above 10 km/s [1]. It is essential to predict gas radiation accurately to

J. M. Lyu (✉) · X. L. Cheng · J. J. Yu
China Academy of Aerospace Aerodynamics, Beijing, China

F. Li · X. L. Yu
Key Laboratory of High Temperature Gas Dynamics, Institute of Mechanics, Chinese Academy of Sciences, Beijing, China

guarantee thermal protection system. Gas radiation calculation is a big challenge for both computations and experiments.

The gas radiation computation involves several physical models, such as fluid dynamics, chemical reactions, thermal non-equilibrium, gas radiation, and radiative transfer. The mathematic models and numerical algorithms are complicated. Generally non-equilibrium flow solvers and delicate spectroscopic models are implemented in radiation calculation, such as LAURA and DPLR for flow and NEQAIR for radiative characteristics [2, 3].

FIRE II project [4] is the first success flight experiment for radiation measurement in which radiative and total heat flux were directly measured using built-in sensors. After FIRE II, there are several flight tests accomplished for thermal protection system under severe conditions of a hyperbolic reentry, such as Stardust in 2006 [5] and Hayabusa in 2010 [6]. However, in these tests, only indirect optical measurements were done. Flight tests for radiation measurement are difficult, expensive, and limited. Till now, FIRE II test data is still the best candidate benchmark for radiation solver validation.

For gas radiation ground experiment, it is hard to conduct the ground test and to measure the radiative flux in small test model. Fortunately, in some high-enthalpy facilities, several basic mechanism experiments counting for chemical reactions and radiation can be carried out to validate the models and methods [7]. In recent 10 years, a number of tests for absolute radiation measurement in Earth/Mars reentry environment have been implemented in EAST of NASA [8, 9], which has given a lot of data to correct the chemical reaction and radiation models. Besides, there are also other similar experiments taken in expansion tubes of Queensland University [10] and shock tube in JAXA Chofu Space Center [11].

In this paper, a series of tests to obtain quantitative emission spectral radiation of air at high velocity have been conducted in a detonation-driven shock tube of the Institute of Mechanics, Chinese Academy of Science. The volumetric spectral radiation of N_2 and air in the spectrum range of 310–380 nm and in the velocity range of 5.5–8 km/s has been acquired. The simulations have also been carried out using an in-house built code to solve the models and equations of gas dynamics and radiation. The comparison between the computation and experiment helped to validate the flow, reactions, and radiation models and to improve the accuracy of radiative heat prediction for reentry vehicles.

2   Models and Methods

2.1   Experiment Setup

A photograph of the shock tube and a demo of the experiment setup are shown in Fig. 1. The facility is a detonation-driven shock tube operated by Prof. Yu in Institute of Mechanics, Chinese Academy of Science [12]. The low-pressure section can be
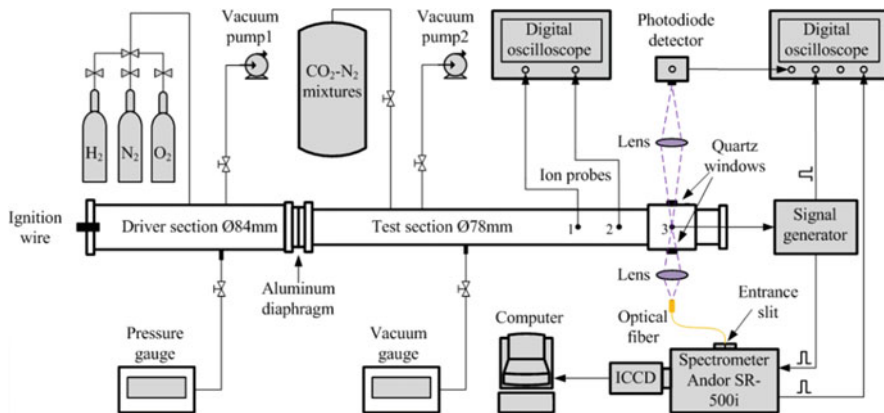
Fig. 1 Demonstration of the shock tube and experiment setup

filled with O_2, N_2, CO_2, or other gases. By adjusting the pressure in the driven section, the shock velocity could cover from 2 to 9 km/s. The relative error of shock velocity in repeated test runs is less than 2%. The calibration was accomplished through a standard optical source before the test shot. The spectrum resolution of the test can be less than 0.1 nm.

2.2 Computation Methods

Generally, gas radiation computation contains four main parts [13]. The first is flowfield solving to obtain the temperature and species number densities. The

second is electronic state population calculation. The third is spectrum calculation to get emission and absorption coefficients in specified frequency range. The last is radiation transport computation to attain the radiative intensity distribution in space and azimuth angles. In the simulation of emission spectral radiation in shock tube, radiative transfer can be neglected.

Navier-Stokes equations with thermochemical non-equilibrium models have been solved to simulate the high-enthalpy flow in front of reentry vehicles. Based on finite volume method on multi-block structured grids, AUSM$^+$-up scheme was used on convection term, where the interface value was obtained by MUSCL method with minmod limiter; second-order central scheme was employed on viscous term; third-order Runge-Kutta method was adopted in time marching; and 11-species and 20-reactions model of air from Gupta [14] was taken to compute chemical reaction sources. The transportation and thermodynamic parameters were calculated through temperature polynomials.

$$\frac{\partial U}{\partial t} + \frac{\partial F}{\partial x} + \frac{\partial G}{\partial y} + \frac{\partial H}{\partial z} = \frac{\partial F_v}{\partial x} + \frac{\partial G_v}{\partial y} + \frac{\partial H_v}{\partial z} + S$$

$$U = \begin{Bmatrix} \rho_i \\ \rho u \\ \rho v \\ \rho w \\ \rho E \end{Bmatrix} \quad F = \begin{Bmatrix} \rho_i u \\ \rho u^2 + p \\ \rho uv \\ \rho uw \\ u(\rho E + p) \end{Bmatrix} \quad G = \begin{Bmatrix} \rho_i v \\ \rho uv \\ \rho v^2 + p \\ \rho vw \\ v(\rho E + p) \end{Bmatrix} \quad H = \begin{Bmatrix} \rho_i w \\ \rho uw \\ \rho vw \\ \rho w^2 + p \\ w(\rho E + p) \end{Bmatrix}$$

$$F_v = \begin{Bmatrix} D_i \frac{\partial \rho_i}{\partial x} \\ \tau_{xx} \\ \tau_{xy} \\ \tau_{xz} \\ \tau_{xx} u + \tau_{xy} v + \tau_{xz} w - q_x \end{Bmatrix} \quad G_v = \begin{Bmatrix} D_i \frac{\partial \rho_i}{\partial y} \\ \tau_{yx} \\ \tau_{yy} \\ \tau_{yz} \\ \tau_{yx} u + \tau_{yy} v + \tau_{yz} w - q_y \end{Bmatrix}$$

$$H_v = \begin{Bmatrix} D_i \frac{\partial \rho_i}{\partial z} \\ \tau_{zx} \\ \tau_{zy} \\ \tau_{zz} \\ \tau_{zx} u + \tau_{zy} v + \tau_{zz} w - q_z \end{Bmatrix} \quad S = \begin{Bmatrix} \dot{w}_i \\ 0 \\ 0 \\ 0 \\ 0 \end{Bmatrix}$$

A narrowband model has been employed to calculate gas radiative characteristics. In these calculations, N_2 first positive band; second positive band; N_2^+ first negative band; NO γ, β, σ, and 1100 nm bands; O_2 Schuman-Runge band; N and O atomic lines and continuum; and N^+ and O^+ continuum radiation are all considered based on electronic transition. The gas absorption coefficients can be calculated by

$$k_\eta = \frac{8\pi^3\eta_0}{3hc}\frac{N'_{e,v,J}R_e^2\left(\overline{r}_{v',v''}\right)q\left(v',v''\right)S_{J''\Lambda''}^{J'\Lambda'}F\left(\eta\right)}{2J''+1}$$

where η_0 is central wave number, h denotes Planck constant, c represents optical velocity, $N'_{e,v,J}$ is number density of low-energy level particles, $R_e\left(\overline{r}_{v',v''}\right)$ is electronic transition matrix of vibrational energy from v' to v'', $q(v',v'')$ is Franck-Condon factor, v' and v'' denote low and high vibrational energy level, $S_{J''\Lambda''}^{J'\Lambda'}$ is intensity factor of rotational spectrum, J and Λ represent quantum number and degeneracy of rotational energy level, and $F(\eta)$ is spectrum line type function.

3 Results and Discussion

First, test data from experiment with N_2 is studied here. In the experiment, the driven section of the shock tube was filled with N_2 at the pressure of 500 Pa. Limited by measure techniques, only one data with a certain time delay can be obtained in one test run. So, generally four test shots have been carried out to get the data with four time delays, which represent four different positions behind the shock. The shock velocities in these four runs were measured to be between 5.46 and 5.7 km/s, which are close.

Standard halogen tungsten lamp was used to calibrate the measurement system, based on which the absolute volumetric radiation intensities of N_2 at 5.5 km/s shock velocity in the spectrum range of 290–340 nm have been obtained for four different time delays. The results are shown in Fig. 2. In these test runs, spectrometer slit width was set to 0.4 mm, the integrating time 500 ns. The corresponding spectrum resolution is 0.25 nm.

The pressure in driving section under the certain shock velocity condition for multispecies reaction gas cannot be simply calculated by general moving shock formula. Therefore, a series of simulation with different driving pressure have been
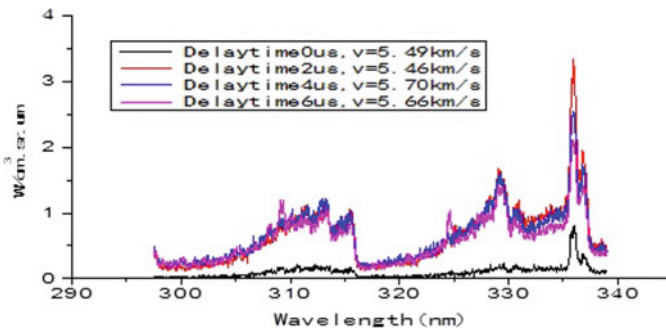

Fig. 2 Measured radiant intensity of N_2 at 5.5 km/s shock velocity with different time delays
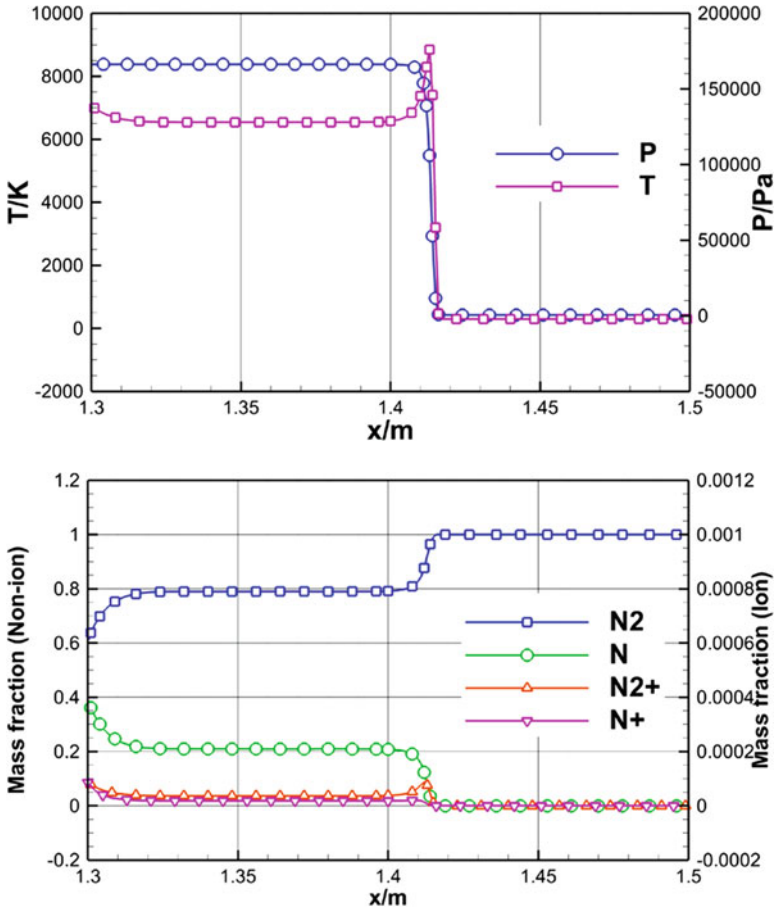
Fig. 3 Computational results of flow parameters and species concentrations of N_2 at 5.5 km/s

implemented. The relation of driving pressure and shock velocity of N_2 under the test condition was found. The computed shock velocity was about 5.5 km/s that came near the measurement value. The flow parameters and species mass concentrations were also acquired in the numerical simulation which are shown in Fig. 3. The peak temperature gets close to 9000 K. Parts of N_2 are dissociated, and a small amount of N_2^+ are produced behind the shock.

The time at which the shock front moved to the position of $x = 1.415$ m was chosen to be the origin. Based on the flow parameters at $x = 1.415$ m when computation time marched forward 2 µs, spectral radiation was calculated. Figure 4 is the comparison of the volumetric spectral radiant intensities between the computation and the test. It is shown that the intensities agree very well. A peak value was noticed near 335 nm in the test result where the computation did not capture. It is believed that this peak radiation is generated by contaminant CN.
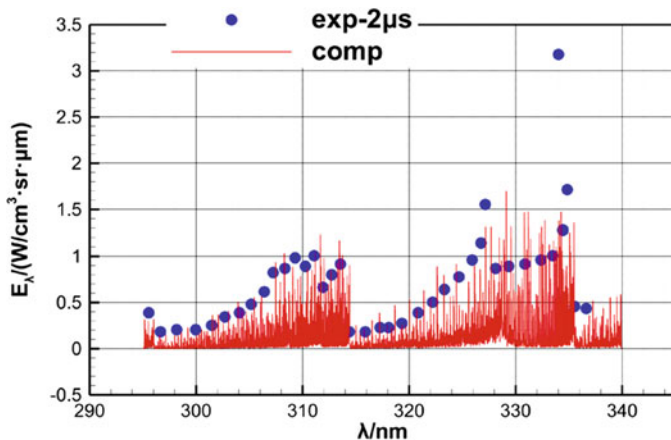
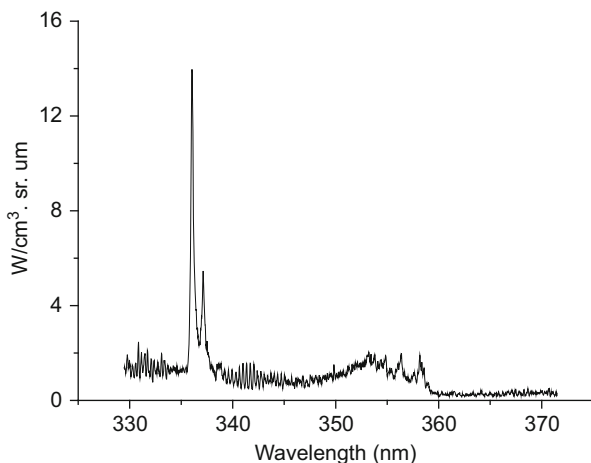**Fig. 4** Comparison between computation and test of N_2 at 5.5 km/s with 2 μs time delay

Fig. 5 Measured radiant intensity of air at 8.1 km/s shock velocity

Then tests of air with faster shock velocity were carried out in which the driven pressure was set to be 20 Pa. The shock velocity was about 8.1 km/s. Under this high-velocity condition, more gas species were present, and more complicated chemical reactions occurred.

Figure 5 is the test results obtained in the spectrum range of 330 and 370 nm. There is also a peak radiation at 335 nm which is emitted by CN in the same way.

The numerical simulations have been performed with 11 species reaction model. The shock velocity calculated in the simulation is about 8.08 km/s which is close to test. Figure 6 is the flow parameters and species mass fractions along the tube. The peak temperature in the shock rises to near 12,000 K. Under this high temperature, O_2 are completely dissociated. The moving shock mainly consist of atom O, N, and ion O^+.
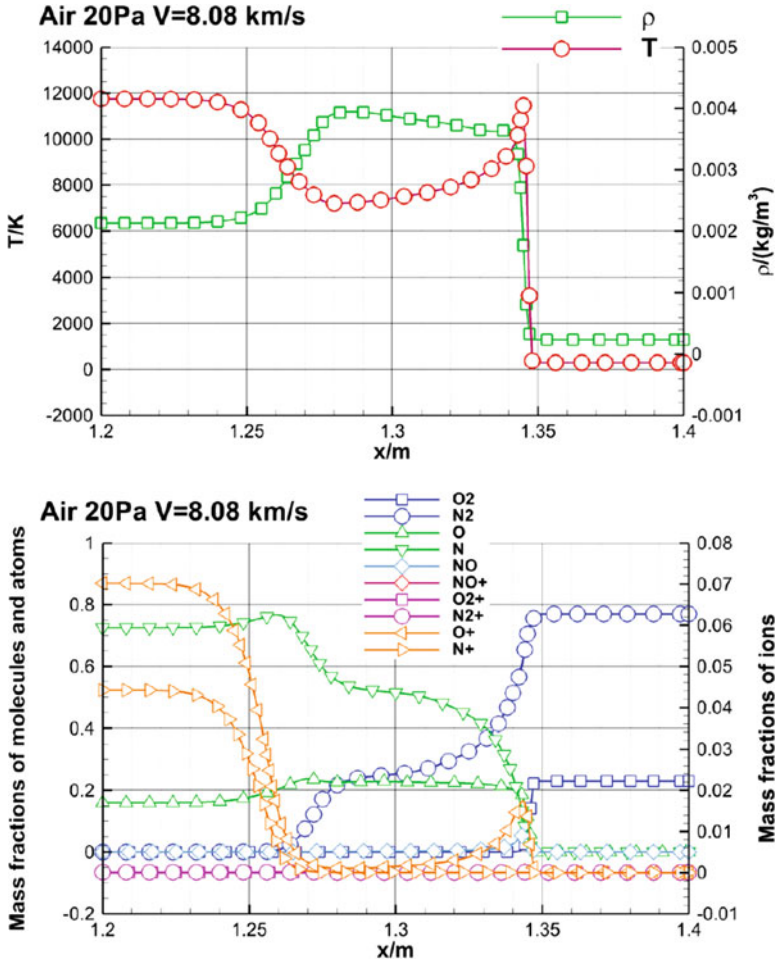
Fig. 6 Flow parameters and species concentrations in shock tube simulation

Figure 7 is the comparison of radiant intensity between the computation results and the test value. The computed radiative intensities agree well with the experiment data like the above N_2 case. It is proved that the flow solver and radiative characteristic calculation are accurate for hyper-velocity and high-temperature gas radiation prediction in shock layer.
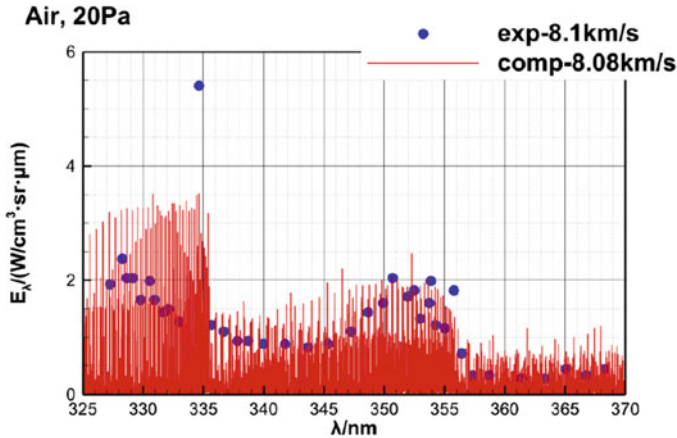
Fig. 7 Comparison of radiant intensity between computation and test of air at 8.1 km/s

4   Conclusion

Spectral radiant intensity of high-temperature gas in shock layer has been studied by both ground experiment and numerical computation. Quantitative radiative intensities of N_2 and air in the visible spectrum range have been acquired in the shock tube with shock velocity from 5.5 to 8.1 km/s. The solving code for multispecies reaction flow and gas radiation has been established, based on which corresponding test cases have been simulated. The results show that the temperature in the shock reaches up to 12,000 K. O^+ and N^+ are produced behind the shock which contribute to the total radiation. The volumetric spectral radiant intensities from the computation and the experiments agree well. It is a guarantee for non-equilibrium flow and gas radiation solver to be used in the future reentry radiative heating prediction.

References

1. J.D. Anderson, An engineering survey of radiating shock layers. AIAA J. **7**(9), 1665–1675 (1969)
2. G.E. Palmer et al., Direct coupling of the NEQAIR radiation and DPLR CFD codes. J. Spacecr. Rocket. **48**(5), 836–845 (2011)
3. D. Hash et al., FIRE II calculations for hypersonic nonequilibrium aerothermodynamics code verification: DPLR, LAURA, and US3D, in *45th AIAA Aerospace Sciences Meeting and Exhibit*, p. 605 (2007)

4. D.L. Cauchon, *Radiative Heating Results from the FIRE II Flight Experiment at a Reentry Velocity of 11.4 Kilometers per Second*. NASA TM X-1402 (1967)
5. I.D. Boyd, P.M. Jenniskens, Modeling of stardust entry at high altitude, part 2: Radiation analysis. J. Spacecr. Rocket. **47**(6), 901–909 (2010)
6. S. Abe et al., Near-ultraviolet and visible spectroscopy of HAYABUSA spacecraft re-entry. Publ. Astron. Soc. Jpn. **63**(5), 1011–1021 (2011)
7. P. Reynier, Survey of high-enthalpy shock facilities in the perspective of radiation and chemical kinetics investigations. Prog. Aerosp. Sci. **85**, 1–32 (2016)
8. A.M. Brandis, B.A. Cruden, Benchmark EAST experiments for earth re-entry, in *55th AIAA Aerospace Sciences Meeting*, p. 1145 (2017)
9. A.M. Brandis et al., Non-equilibrium radiation for earth entry, in *46th AIAA Thermophysics Conference*, p. 3690 (2016)
10. S.W. Lewis et al., Expansion tunnel experiments of earth reentry flow with surface ablation. J. Spacecr. Rocket. **53**(5), 887–899 (2016)
11. H. Takayanagi, K. Fujita, Absolute radiation measurements behind strong shock wave in carbon dioxide flow for mars aerocapture missions, in *43rd AIAA Thermophysics Conference*, p. 2744 (2012)
12. X. Lin et al., Measurements of non-equilibrium and equilibrium temperature behind a strong shock wave in simulated Martian atmosphere. Acta Mech. Sinica **28**, 5 (2012)
13. C.O. Johnston, *Nonequilibrium Shock-Layer Radiative Heating for Earth and Titan Entry*, Ph.D. Thesis, Virginia Polytechnic Institute and State University, Blacksburg, 2006
14. R.N. Gupta et al., *A Review of Reaction Rates and Thermodynamic and Transport Properties for an 11-Species Air Model for Chemical and Thermal Nonequilibrium Calculations to 30000 K*. NASA STI/Recon Technical Report N, 90, 27064 (1990)